Note on the calculation of the bacterial production (BP)

Leucine incorporation rates were calculated using Eq. (1):

$$Leu_{Inc} = \frac{DPM \times 4.5 \times 10^{-13}}{SA \times t \times V}, \quad (1)$$

where Leu_{Inc} is the sample leucine incorporation in mmol leucine L^{-1} h^{-1}, DPM is the sample corrected DPM, 4.5 x 10^{-13} is a constant in Ci DPM^{-1}, SA is the specific activity of leucine in Ci $mmol^{-1}$, t is the incubation time in hours, and V is the volume of the sample in litres. BP was expressed as the production of carbon biomass calculated from leucine incorporation using the coefficients and Eq. (2) from Simon and Azam (1989):

$$BP = Leu_{Inc} \times 131.2 \div 0.073 \times 0.86 \times ID \times 10^3, \quad (2)$$

where BP is the bacterial carbon production in µgC L^{-1} h^{-1}, Leu_{Inc} is the sample leucine incorporation in mmol leucine L^{-1} h^{-1}, 131.2 is the molecular weight of leucine in g mol^{-1}, 0.073 is the fraction of leucine in proteins, 0.86 is the fraction of carbon in proteins, and ID is the isotope dilution value. As ID was not specifically estimated, the conservative value of 1 was used as advised by Kirchman (2001).

Table S1. Additional limnological data from the winter sampling in 2016, including temperature, dissolved oxygen (DO), pH, conductivity, total phosphorus (TP), total nitrogen (TN), total iron (Fe), dissolved organic carbon (DOC), DOM absorption coefficient at 320 nm (a_{320}), DOM specific UV absorbance at 254 nm ($SUVA_{254}$), DOM spectral slope between 275 and 295 nm (S_{285}), total fluorescence of DOM (F_{tot}), and the amount of fluorescence for each of the five components retrieved by PARAFAC (C1-C5). Values are given at three depths under the ice cover as sampled on 19 March (over a total water column of about 1.7 m). DOM characteristics of the water collected for the experiment at the surface on 24 March are also given for comparison. Temperature, DO, pH and conductivity profiles were obtained using a multiparameter probe (Hydrolab DS5X, OTT HydroMet GmbH, Germany; temperature ± 0.1°C, polarographic DO ± 0.6 mg L^{-1}, pH ± 0.2 units, conductivity ± 0.001 mS cm^{-1}). Water for the quantification of DOC and DOM properties was filtered in the field on pre-rinsed 0.2-µm cellulose acetate filters. TP, TN, cations and DOC were analysed as described in (Bouchard et al., 2015). Values of a_{320}, $SUVA_{254}$ and S_{285} were computed from 250-800 nm absorbance spectra, while the five components of fluorescing DOM were extracted using the PARAFAC model (described in the method section of the article).

	Depth under the ice cover (m)			
	19 March			24 March
	0 (surface)	0.5	1.3 (bottom)	0 (surface)
Temperature (°C)	0.5	0.6	1.9	NA
DO (mg L^{-1})	0.0	0.0	0.0	NA
pH	5.00	5.00	5.10	NA
Conductivity (µS cm^{-1})	69	69	91	NA
TP (µg P L^{-1})	11	21	31	NA
TN (mg N L^{-1})	1.25	1.35	1.44	NA
Fe (mg L^{-1})	3.0	3.1	3.9	NA
DOC (mgC L^{-1})	18.3	19.5	20.9	19.2
a_{320} (m^{-1})	142	157	169	144
$SUVA_{254}$ (L mgC^{-1} m^{-1})	6.78	6.98	6.85	6.51
S_{285} (nm^{-1})	0.0111	0.0109	0.0105	0.0110
F_{tot} (RU)	4.9	5.5	5.2	5.0
C1 (RU)	2.0	2.1	2.0	1.9
C2 (RU)	1.4	1.6	1.6	1.4
C3 (RU)	0.6	0.6	0.6	0.6
C4 (RU)	0.5	0.4	0.3	0.4
C5 (RU)	0.6	0.7	0.8	0.7

Table S2. Description of the five fluorescent components identified with the PARAFAC model. Secondary peaks are indicated in parentheses. The comparison with the literature was done on Openfluor using the criteria of the Tucker congruence coefficient (TCC).

PARAFAC component	Excitation peaks (nm)	Emission peaks (nm)	Matching score	Examples of matching in literature	Attributed characteristics
C1	< 250 (340)	478	TCC > 0.95 > 30 models	- Williams et al., 2010: C1, streams - Osburn et al., 2016: C1, coastal and estuarine waters - Yamashita et al., 2010: C1, subtropical wetlands	Ubiquitous humic-like, terrestrial origin
C2	< 250 (310)	432	0.90 < TCC < 0.95 2 models	-Williams et al., 2010: C2, bio-refractory - Søndergaard et al., 2003: C1, wetland and forest drainage waters	Humic-like terrestrial origin
C3	< 250 (300, 390)	512	TCC > 0.95 > 30 models	- Osburn et al., 2012: C1, estuaries - Stedmon et al., 2007: C2, seawater - Graeber et al., 2012: C2, agricultural, forested and wetland catchments - Kida et al., 2019: C4, Antarctic water, autochthonous	Humic-like, presumable terrestrial origin
C4	270	406	0.90 < TCC < 0.95 1 model	- Dainard et al., 2015: C5, Beaufort Sea, photodegradable	Humic-like
C5	280 (350)	444	TCC > 0.95 4 models	- Lapierre and del Giorgio, 2014: C3, boreal region, extremely photodegradable - Murphy et al., 2018 : C2, ubiquitous and photodegradable	Humic-like

Table S3. Summary of the ANOVAs showing the effects of the full factorial design, including factors Time, Light and Bacteria for all variables of interest.

Source of variation	df	F ratio	P
(a) DIC			
Time	3	13.3	< 0.0001
Light	1	756.4	< 0.0001
Time*Light	3	15.0	< 0.0001
Bacteria	1	0.4	0.5195
Time*Bacteria	3	4.3	0.0117
Light*Bacteria	1	17.2	0.0002
Time*Light*Bacteria	3	1.7	0.1916
(b) DOC			
Time	3	232.1	< 0.0001
Light	1	3215.8	< 0.0001
Time*Light	3	165.0	< 0.0001
Bacteria	1	6.0	0.0201
Time*Bacteria	3	3.9	0.0172
Light*Bacteria	1	44.7	< 0.0001
Time*Light*Bacteria	3	5.2	0.0050
(c) a_{320}			
Time	3	124.3	< 0.0001
Light	1	2333.8	< 0.0001
Time*Light	3	106.4	< 0.0001
Bacteria	1	15.5	0.0004
Time*Bacteria	3	2.9	0.0499
Light*Bacteria	1	9.0	0.0052
Time*Light*Bacteria	3	4.9	0.0062
(d) S_{285}			
Time	3	53.0	< 0.0001
Light	1	2127.0	< 0.0001
Time*Light	3	51.0	< 0.0001
Bacteria	1	6.3	0.0177
Time*Bacteria	3	1.7	0.1796
Light*Bacteria	1	6.1	0.0189
Time*Light*Bacteria	3	2.2	0.1117
(e) $SUVA_{254}$			
Time	3	16.0	< 0.0001
Light	1	13.8	0.0008
Time*Light	3	28.3	< 0.0001
Bacteria	1	60.2	< 0.0001
Time*Bacteria	3	5.0	0.0059
Light*Bacteria	1	84.3	< 0.0001
Time*Light*Bacteria	3	9.1	0.0002
(f) F_{tot}			
Time	3	274.2	< 0.0001
Light	1	21037.9	< 0.0001
Time*Light	3	689.0	< 0.0001
Bacteria	1	147.9	< 0.0001
Time*Bacteria	3	1.9	0.1504
Light*Bacteria	1	143.3	< 0.0001
Time*Light*Bacteria	3	1.6	0.2084
(g) C1			
Time	3	57.6	< 0.0001
Light	1	2983.0	< 0.0001
Time*Light	3	129.9	< 0.0001
Bacteria	1	36.1	< 0.0001
Time*Bacteria	3	2.1	0.1143
Light*Bacteria	1	37.9	< 0.0001
Time*Light*Bacteria	3	1.4	0.2649

Table S3. Continued.

Source of variation	df	F ratio	P
(h) C2			
Time	3	102.1	< 0.0001
Light	1	3253.4	< 0.0001
Time*Light	3	228.7	< 0.0001
Bacteria	1	69.8	< 0.0001
Time*Bacteria	3	2.0	0.1368
Light*Bacteria	1	147.0	< 0.0001
Time*Light*Bacteria	3	2.2	0.1064
(i) C3			
Time	3	237.1	< 0.0001
Light	1	35475.3	< 0.0001
Time*Light	3	583.0	< 0.0001
Bacteria	1	20.4	< 0.0001
Time*Bacteria	3	0.8	0.5099
Light*Bacteria	1	8.8	0.0057
Time*Light*Bacteria	3	5.4	0.0042
(j) C4			
Time	3	89.9	< 0.0001
Light	1	187.3	< 0.0001
Time*Light	3	46.1	< 0.0001
Bacteria	1	39.5	< 0.0001
Time*Bacteria	3	0.8	0.4884
Light*Bacteria	1	69.1	< 0.0001
Time*Light*Bacteria	3	2.9	0.0510
(k) C5			
Time	3	17.7	< 0.0001
Light	1	5731.8	< 0.0001
Time*Light	3	77.5	< 0.0001
Bacteria	1	0.1	0.8325
Time*Bacteria	3	1.8	0.1734
Light*Bacteria	1	2.6	0.1180
Time*Light*Bacteria	3	1.4	0.2657
(l) BA			
Time	3	42.5	< 0.0001
Light	1	352.8	< 0.0001
Time*Light	3	36.8	< 0.0001
Bacteria	1	68.1	< 0.0001
Time*Bacteria	3	69.7	< 0.0001
Light*Bacteria	1	93.5	< 0.0001
Time*Light*Bacteria	3	46.2	< 0.0001
(n) BP			
Time	3	1.3	0.2652
Light	1	39.0	< 0.0001
Time*Light	3	0.1	0.8297
Bacteria	1	77.6	< 0.0001
Time*Bacteria	3	10.3	0.0058
Light*Bacteria	1	0.8	0.3872
Time*Light*Bacteria	3	1.7	0.2143
(o) Normalized BP			
Time	3	13.5	0.0023
Light	1	0.1	0.8281
Time*Light	3	0.2	0.6648
Bacteria	1	33.8	< 0.0001
Time*Bacteria	3	7.0	0.0184
Light*Bacteria	1	0.1	0.8198
Time*Light*Bacteria	3	5.9	0.0285

Table S4. Summary of the ANOVAs showing the effects of the full factorial design including factors Time and Treatment, for all variables of interest.

Source of variation	df	F ratio	P-value
(a) DIC			
Time	3	10.1	< 0.0001
Treatment	4	266.0	< 0.0001
Time*Treatment	12	6.9	< 0.0001
(b) DOC			
Time	3	244.7	< 0.0001
Treatment	4	981.7	< 0.0001
Time*Treatment	12	62.5	< 0.0001
(c) a_{320}			
Time	3	133.9	< 0.0001
Treatment	4	870.4	< 0.0001
Time*Treatment	12	45.5	< 0.0001
(d) S_{285}			
Time	3	49.5	< 0.0001
Treatment	4	666.7	< 0.0001
Time*Treatment	12	21.2	< 0.0001
(e) $SUVA_{254}$			
Time	3	15.1	< 0.0001
Treatment	4	45.3	< 0.0001
Time*Treatment	12	13.9	< 0.0001
(f) F_{tot}			
Time	3	359.4	< 0.0001
Treatment	4	6588.4	< 0.0001
Time*Treatment	12	258.7	< 0.0001
(g) C1			
Time	3	74.1	< 0.0001
Treatment	4	959.0	< 0.0001
Time*Treatment	12	50.0	< 0.0001
(h) C2			
Time	3	144.9	< 0.0001
Treatment	4	1122.4	< 0.0001
Time*Treatment	12	88.3	< 0.0001
(i) C3			
Time	3	198.8	< 0.0001
Treatment	4	9804.6	< 0.0001
Time*Treatment	12	191.7	< 0.0001
(j) C4			
Time	3	174.4	< 0.0001
Treatment	4	99.8	< 0.0001
Time*Treatment	12	19.8	< 0.0001
(k) C5			
Time	3	15.6	< 0.0001
Treatment	4	1778.0	< 0.0001
Time*Treatment	12	27.7	< 0.0001
(l) BA			
Time	3	43.4	< 0.0001
Treatment	4	152.8	< 0.0001
Time*Treatment	12	38.0	< 0.0001
(m) BP			
Time	3	0.5	0.5127
Treatment	4	36.6	< 0.0001
Time*Treatment	12	3.3	0.0332
(n) Normalized BP			
Time	3	14.4	0.0012
Treatment	4	10.4	0.0001
Time*Treatment	12	4.1	0.0151

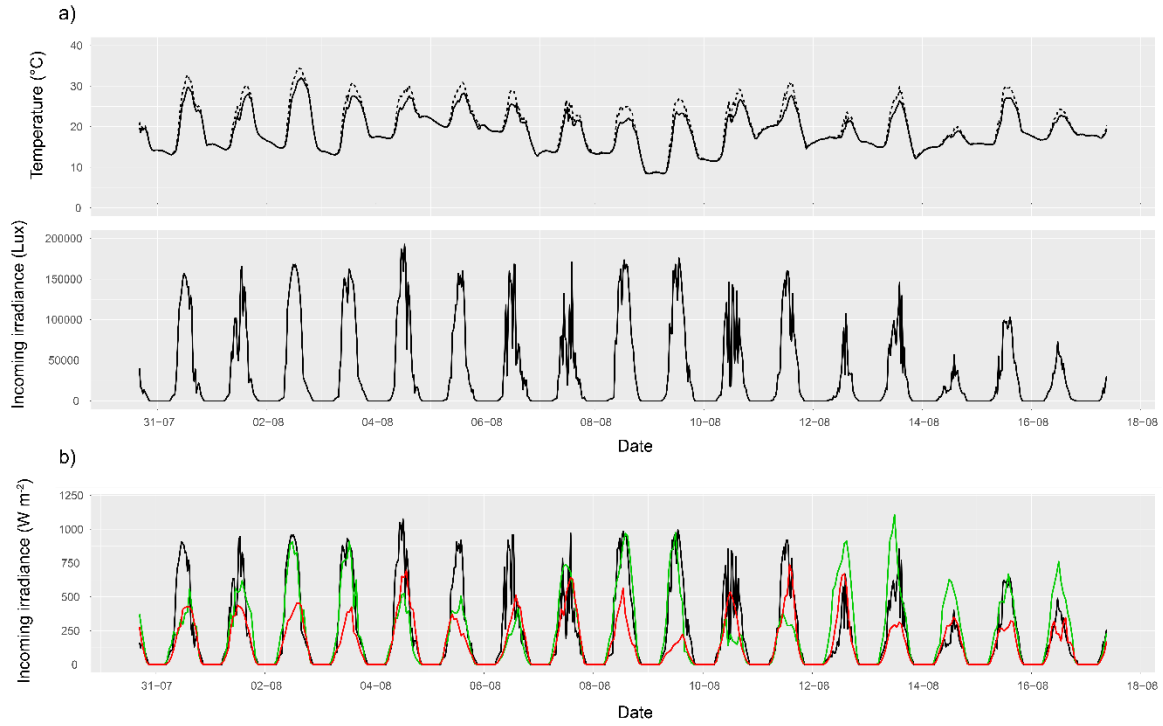

Figure S1. Data from the Pendant sensors installed in the incubation tray (a). The top graph is showing the temperature of the sensor exposed to sunlight (light treatment, dashed line) or wrapped in black tape (dark treatment, continuous line). The bottom graph presents incoming irradiance (in Lux) as a relative measurement of incoming irradiance. As the incubation was conducted outside, the water temperature and irradiance received by the samples depended on local meteorological conditions. The incoming irradiance (b) received at Quebec City during the experimental period (black line) is compared to irradiance received at the nearby village of Whapmagoostui- Kuujjuarapik (green line – mean over 2015 and 2016; CEN, 2020a) and at the study site SAS (red line – mean over 2017, 2018 and 2019; CEN, 2020b). Irradiance was not yet available at SAS in August 2016. Irradiance data at Quebec City come from Laval University station, with the three first days reconstructed from Pendant data as explained in the methods section.

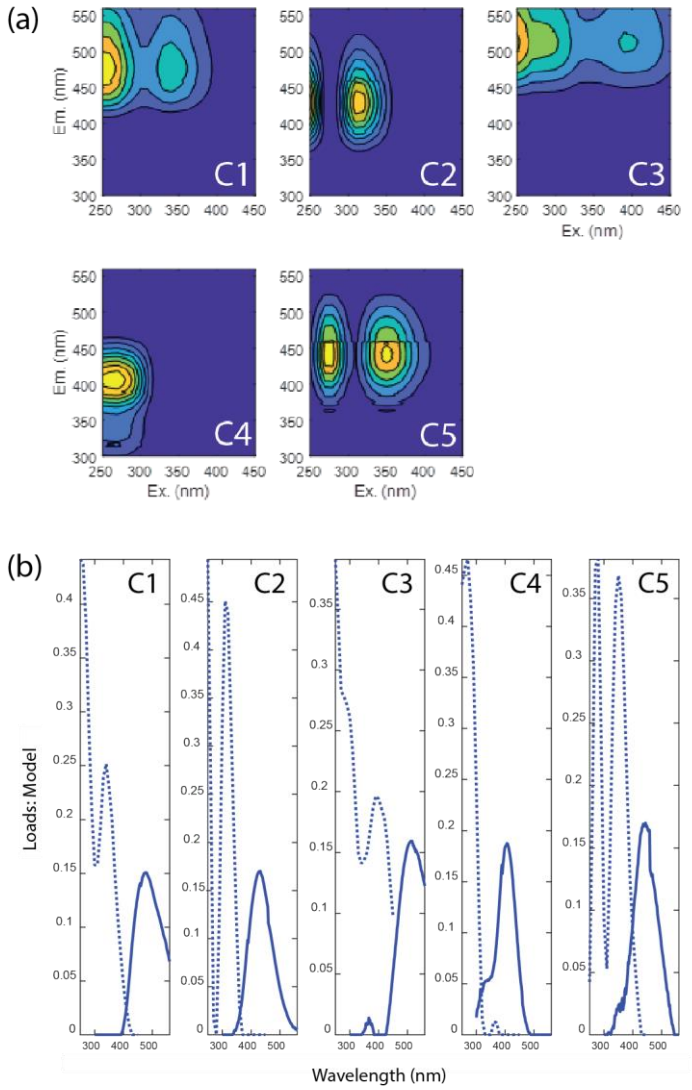

Figure S2. The fingerprints (a) and loadings (b) of the five fluorescent components identified by the PARAFAC model (C1-C5). In (b), dashed and full lines respectively represent excitation and emission spectra.

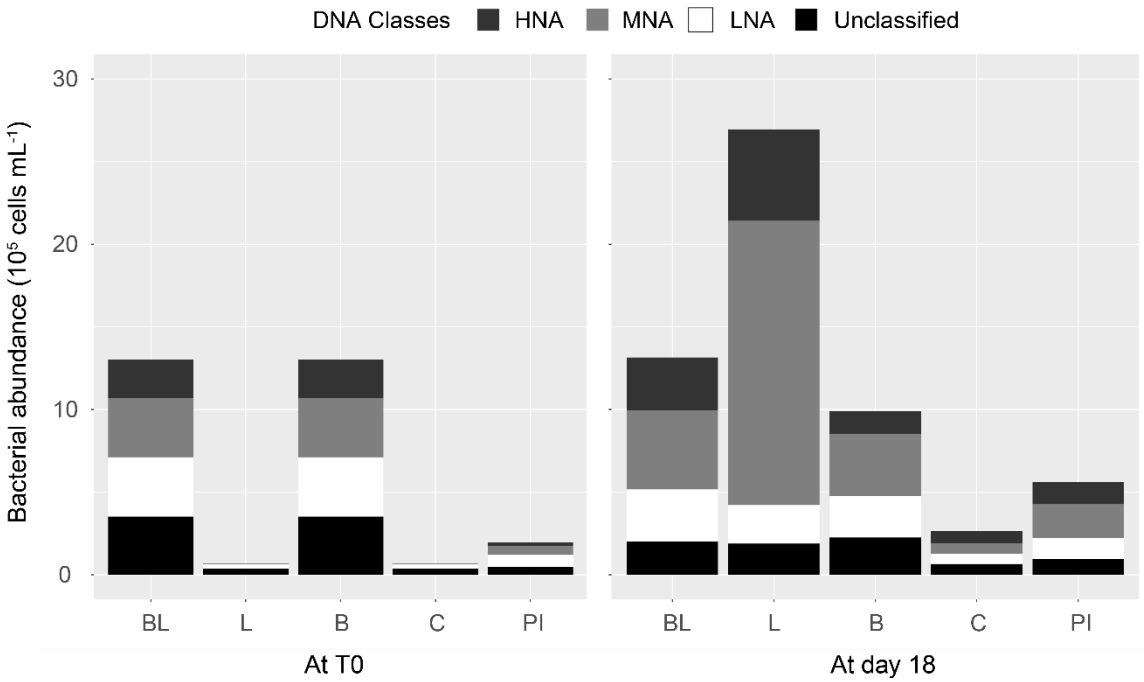

Figure S3. Repartition of the total bacterial abundance (BA) among the low (LNA), medium (MNA) and high (HNA) DNA populations identified by cytometric gating. Unclassified bacteria that did not belong to any of these three populations are also shown. Refer to Figure S4 for gating examples.

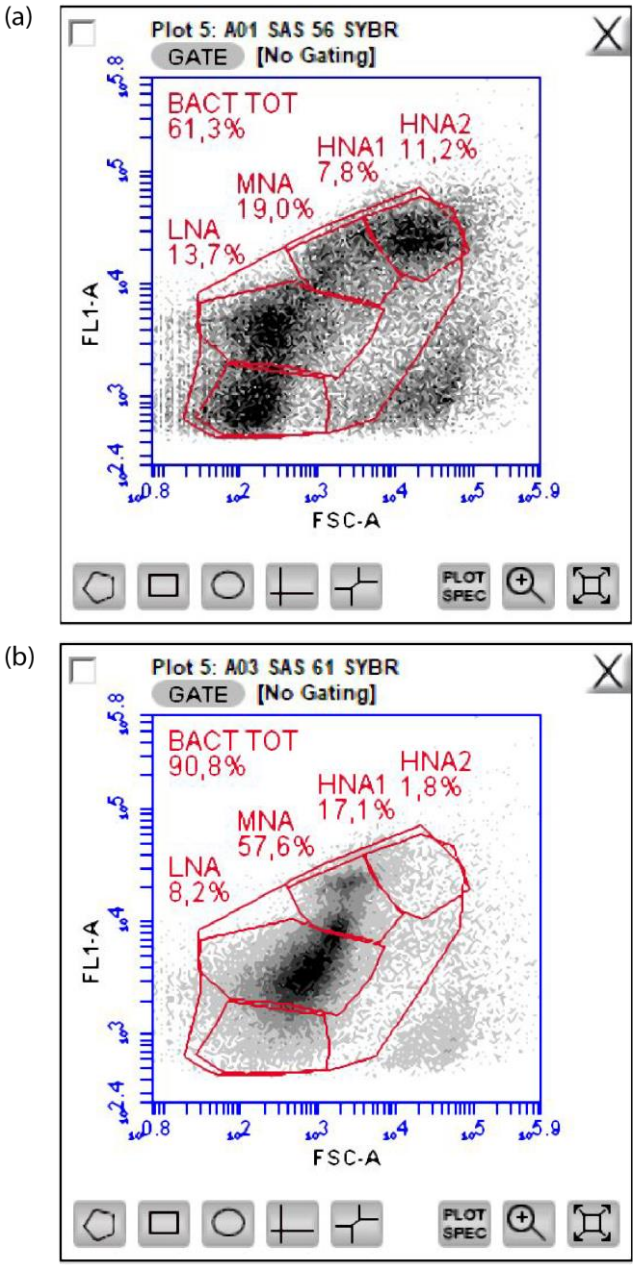

Figure S4. Examples of the cytometric gating used for the extraction of the bacterial abundance. Low (LNA), medium (MNA) and high (HNA) DNA populations were defined as massive group of cells discriminated on the strength of the green fluorescence signal. Note that HNA = HNA1 + HNA2. The cytogram (a) is from a sample of the BL treatment at 18 days. The cytogram (b) shows the two massive populations that emerged in samples of the L treatment after 18 days of incubation.

References cited

Bouchard, F., Laurion, I., Preskienis, V., Fortier, D., Xu, X. and Whiticar, M. J.: Modern to millennium-old greenhouse gases emitted from ponds and lakes of the Eastern Canadian Arctic (Bylot Island, Nunavut), Biogeosciences, 12(23), 7279–7298, doi:10.5194/bg-12-7279-2015, 2015.

Centre for northern studies (CEN): Climate station data from Whapmagoostui-Kuujjuarapik Region in Nunavik, Quebec, Canada, v. 1.5 (1987-2019). Nordicana D4, 2020a.

Centre for northern studies (CEN): Unpublished data, 2020b.

Dainard, P. G., Guéguen, C., McDonald, N. and Williams, W. J.: Photobleaching of fluorescent dissolved organic matter in Beaufort Sea and North Atlantic Subtropical Gyre, Mar. Chem., 177, 630–637, doi:10.1016/j.marchem.2015.10.004, 2015.

Graeber, D., Gelbrecht, J., Pusch, M. T., Anlanger, C. and von Schiller, D.: Agriculture has changed the amount and composition of dissolved organic matter in Central European headwater streams, Sci. Total Environ., 438, 435–446, doi:10.1016/j.scitotenv.2012.08.087, 2012.

Kida, M., Kojima, T., Tanabe, Y., Hayashi, K., Kudoh, S., Maie, N. and Fujitake, N.: Origin, distributions, and environmental significance of ubiquitous humic-like fluorophores in Antarctic lakes and streams, Water Res., 163, 114901, doi:10.1016/j.watres.2019.114901, 2019.

Kirchman, D.: Measuring bacterial biomass production and growth rates from leucine incorporation in natural aquatic environments, in Methods in Microbiology, vol. 30, edited by J. H. Paul, pp. 227–237, Academic Press. [online] Available from: https://www.sciencedirect.com/science/article/pii/S0580951701300478, 2001.

Lapierre, J.-F. and del Giorgio, P. A.: Partial coupling and differential regulation of biologically and photochemically labile dissolved organic carbon across boreal aquatic networks, Biogeosciences, 11, 5969–5985, doi:10.5194/bg-11-5969-2014, 2014.

Murphy, K. R., Timko, S. A., Gonsior, M., Powers, L. C., Wünsch, U. J. and Stedmon, C. A.: Photochemistry Illuminates Ubiquitous Organic Matter Fluorescence Spectra, Environ. Sci. Technol., 52, 11243–11250, doi:10.1021/acs.est.8b02648, 2018.

Osburn, C. L., Handsel, L. T., Mikan, M. P., Paerl, H. W. and Montgomery, M. T.: Fluorescence Tracking of Dissolved and Particulate Organic Matter Quality in a River-Dominated Estuary, Environ. Sci. Technol., 46, 8628–8636, doi:10.1021/es3007723, 2012.

Osburn, C. L., Boyd, T. J., Montgomery, M. T., Bianchi, T. S., Coffin, R. B. and Paerl, H. W.: Optical Proxies for Terrestrial Dissolved Organic Matter in Estuaries and Coastal Waters, Front. Mar. Sci., 2(127), doi:10.3389/fmars.2015.00127, 2016.

Simon, M. and Azam, F.: Protein content and protein synthesis rates of planktonic marine bacteria, Mar. Ecol. Prog. Ser., 51, 201–213, 1989.

Søndergaard, M., Stedmon, C. A. and Borch, N. H.: Fate of terrigenous dissolved organic matter (DOM) in estuaries: Aggregation and bioavailability, Ophelia, 57(3), 161–176, doi:10.1080/00785236.2003.10409512, 2003.

Stedmon, C. A., Thomas, D. N., Granskog, M., Kaartokallio, H., Papadimitriou, S. and Kuosa, H.: Characteristics of Dissolved Organic Matter in Baltic Coastal Sea Ice: Allochthonous or Autochthonous Origins?, Environ. Sci. Technol., 41(21), 7273–7279, doi:10.1021/es071210f, 2007.

Williams, C. J., Yamashita, Y., Wilson, H. F., Jaffe, R. and Xenopoulos, M. A.: Unraveling the role of land use

and microbial activity in shaping dissolved organic matter characteristics in stream ecosystems, Limnol. Oceanogr., 55(3), 1159–1171, doi:10.4319/lo.2010.55.3.1159, 2010.

Yamashita, Y., Scinto, L. J., Maie, N. and Jaffé, R.: Dissolved Organic Matter Characteristics Across a Subtropical Wetland's Landscape: Application of Optical Properties in the Assessment of Environmental Dynamics, Ecosystems, 13(7), 1006–1019, doi:10.1007/s10021-010-9370-1, 2010.